1   Functional assays for the assessment of the pathogenicity of variants in GOSR2, an

2   ER-to-Golgi SNARE involved in progressive myoclonus epilepsies

3

4

5   Jörn M. Völker[1], Mykola Dergai[2], Luciano A. Abriata[3], Yves Mingard[2], Daniel Ysselstein[4], Dimitri

6   Krainc[4], Matteo Dal Peraro[3], Gabriele Fischer von Mollard[1], Dirk Fasshauer[2], Judith Koliwer[1,*] and

7   Michael Schwake[1,4*]

8

9

10   [1] *Biochemistry III/ Faculty of Chemistry, Bielefeld University, Universitätsstr. 25, 33615 Bielefeld,*
11   *Germany*
12   [2] *Department of Fundamental Neurosciences, University of Lausanne, Rue du Bugnon 9, 1005*
13   *Lausanne, Switzerland*
14   [3] *Institute of Bioengineering, School of Life Sciences, École Polytechnique Fédérale de Lausanne*
15   *(EPFL), CH-1015 Lausanne, Switzerland and Swiss Institute of Bioinformatics (SIB), CH-1015*
16   *Lausanne, Switzerland.*
17   [4] *Department of Neurology, Northwestern University Feinberg School of Medicine, 303 East Chicago*
18   *Avenue, 60611 Chicago, USA*
19   ** Correspondence should be addressed to M.S. (schwake@northwestern.edu) or J.K.*
20   *(judith.koliwer@uni-bielefeld.de)*

21

24

25

26   **Abbreviations and nomenclature**

27   Progressive myoclonus epilepsies (PME), Golgi SNAP receptor complex member 2

28   (GOSR2),

29

30   **Keywords**

31   Progressive myoclonus epilepsies, PME, GOSR2, membrin, GS27, Bos1

32

33   **Running title**

34   Functionality of GOSR2 mutants

35

36   **Summary statement**

37   Mutations in the Qb-SNARE GOSR2 cause progressive myoclonus epilepsies. We report the

38   effect of two mutations on SNARE function to investigate the correlation with progression and

39   severity of disease.

40

Abstract

42 Progressive myoclonus epilepsies (PME) are inherited disorders characterized by
43 myoclonus, generalized tonic-clonic seizures, and ataxia. One of the genes that are
44 associated with PME is the ER-to-Golgi Q_b-SNARE GOSR2, **which forms** a SNARE
45 complex with Syntaxin5, Bet1 and Sec22b. Most PME patients are homozygous for **a**
46 p.Gly144Trp mutation and develop similar clinical presentations. **Recently, a patient who**
47 **was compound heterozygous for the p.Gly144Trp and a novel p.Lys164del mutation**
48 **was identified. Since this patient presented with a milder disease phenotype, we**
49 **hypothesized that the p.Lys164del mutation may be less severe compared to**
50 **p.Gly144Trp. To characterize** the effect of the p.Gly144Trp and p.Lys164del mutations**,**
51 both of which are present in the SNARE motif of GOSR2, we examined the corresponding
52 mutations in the yeast orthologue Bos1. Yeasts expressing the orthologous mutants in Bos1
53 showed impaired growth, suggesting a partial loss of function, which was more severe for the
54 Bos1 p.Gly176Trp mutation. Using anisotropy and gel filtration, we report that Bos1
55 p.Gly176Trp and p.Arg196del are capable of complex formation, however with partly reduced
56 activity. Molecular dynamics simulations showed that the hydrophobic core, which triggers
57 SNARE complex formation, is compromised due to the glycine to tryptophan substitution in
58 both GOSR2 and Bos1. In contrast, the deletion of residue p.Lys164 (or p.Arg196del in
59 Bos1) interferes with the formation of hydrogen bonds between GOSR2 and Syntaxin5.
60 Despite these perturbations, all SNARE complexes stayed intact during longer simulations.
61 Thus, our data suggest that the mild**er** course of disease in compound heterozygous PME is
62 due to less severe impairment of the SNARE function.

63

Introduction

65 Subcellular trafficking of membranes and their associated proteins is essential for proper
66 function of eukaryotic cells. Fission from donor membranes and fusion of transport vesicles
67 with target membranes allows for controlled transport of cargo including lipids, proteins, and
68 cellular messengers such as hormones. SNARE (soluble NSF [N-ethylmaleimide-sensitive
69 factor] attachment protein receptor) proteins, with their highly conserved SNARE domains,
70 are a main component of the fusion process. Four different SNARE domains found on
71 vesicles and target membranes interact to form a quaternary SNARE complex providing the
72 driving force necessary for membrane fusion (Jahn and Scheller, 2006). The SNARE
73 complex structure is defined by a twisted parallel bundle of four helices (Sutton et al., 1998).
74 The contacting surfaces of these helices can be separated into 16 layers which are indicated

75 by numbers from -7 to +8 (Fig. 1). These layers are mainly hydrophobic, except for the

76 hydrophilic 0-layer in the center of the bundle (Fasshauer et al., 1998a). The complex usually

77 consists of three Q-SNAREs (Q_a, Q_b and Q_c) and one R-SNARE, which contain a glutamine

78 or an arginine in the 0-position, respectively (Fasshauer et al., 1998b).

79 One of the earliest membrane fusion events in the secretory pathway is the anterograde

80 transport between endoplasmic reticulum (ER) and Golgi. In this step, the Q_b-SNARE

81 GOSR2, also referred to as membrin or GS27, forms a complex with the Q_a-SNARE

82 Syntaxin5, the Q_c-SNARE Bet1, and the R-SNARE Sec22b (Hay et al., 1997, Lowe et al.,

83 1997). This SNARE complex appears to mediate several fusion processes between the ER,

84 the ER-Golgi intermediate compartment (ERGIC), and the Golgi (Hay et al., 1998). The

85 importance of GOSR2 in these processes is supported by the observations that knockdown

86 of GOSR2 leads to a significant decrease in transport from ER to Golgi and interferes with

87 Golgi maintenance (Gordon et al., 2010, Lowe et al., 1997). The structural, kinetic, and

88 regulatory mechanisms of the complex formation are unknown, although it is likely that the R-

89 SNARE Sec22b interacts with a preformed ternary complex of all three Q-SNAREs (Xu et al.,

90 2000). It is **also** likely that this process is highly regulated as studies with yeast SNAREs *in*

91 *vitro* have revealed that membrane fusion occurs only when Bet1 is located on a donor

92 membrane and its SNARE partners are on an acceptor membrane (Parlati et al., 2000).

93 Mutations in GOSR2 are associated with progressive myoclonus epilepsies (PME),

94 characterized by myoclonus, generalized tonic clonic seizures, and ataxia (Berkovic et al.,

95 1986). A group of PME patients has been identified to possess a homozygous mutation

96 c.430G>T in the gene encoding for GOSR2 on chromosome 17, resulting in a p.Gly144Trp

97 substitution in the protein. Glycine 144 is localized in the conserved SNARE domain of the

98 protein. This homozygous mutation was first detected in a PME patient with severe motor

99 disturbance with no described development of dementia. However, in autopsy a slightly

100 reduced weight of the brain was measured and minor loss of Purkinje cells and gliosis in the

101 cerebellar vermis were detected (Corbett et al., 2011). With time, 11 more patients were

102 found to possess the p.Gly144Trp variant of GOSR2. The syndrome was called "North Sea

103 PME" given the fact that all patients originated from countries surrounding the North Sea

104 (Boisse Lomax et al., 2013). These patients shared a similar phenotype with an onset of

105 ataxia of about 2 years, onset of myoclonic seizures of about 6.5 years, and scoliosis by

106 adolescence. The patients also do not display significant intellectual disability or cognitive

107 dysfunction until late in disease progression.

108 Recently, a case of PME was reported in a female patient with compound heterozygous

109 mutation**s** in the gene encoding for GOSR2 (Praschberger et al., 2015). This patient carried

110 the already described p.Gly144Trp mutation on one allele, whereas the other allele carried a

111 novel in-frame deletion of three base pairs c.491_493delAGA. This deletion results in loss of

112 a lysine (p.Lys164del), which **is located** within the SNARE domain of GOSR2. The
113 respective patient was 61 years old and displayed a rather mild disease course **with only**
114 **mild cognitive dysfunction** compared to patients homozygous for the p.Gly144Trp
115 mutation. **These observations** suggest that the deletion of the lysine residue at position 164
116 has less severe functional consequences than the p.Gly144Trp mutation. Therefore, in this
117 study we aimed to understand the functional effect of the two PME linked mutations in
118 GOSR2 and their influence on the stability and formation of the SNARE complex necessary
119 for ER-to-Golgi transport.

120

121 **Results**

122 **The deletion of arginine 196 in Bos1 leads to a partial loss of function in yeast.**

123 **T**he **more** mild disease course of **the** patient **that is** compound heterozygous for the
124 p.Gly144Trp and the p.Lys164del in GOSR2 and the lack of functional data on the
125 p.Lys164del mutation, **prompted us** to functionally characterize these mutations in more
126 detail. Both mutations reside in the SNARE domain of GOSR2 (Fig. 1), and therefore
127 possibly affect SNARE complex assembly and/or function. The 16 layers of the SNARE
128 domain of GOSR2 display remarkably evolutionary conservation in the animal kingdom **and**
129 **in** the orthologous protein in fungi called Bos1. Sequence alignment of human GOSR2 and
130 Bos1 from *Saccharomyces cerevisiae* indicates conservation of the p.Gly144/p.Gly176 and
131 similarity of the p.Lys164/p.Arg196 amino acids (Fig**.** 1). The p.Gly144/p.Gly176 residues are
132 located within the -3 layer in the SNARE domain of both GOSR2 and BOS1, while the
133 p.Lys164 and p.Arg196 residues reside between layer +2 and +3, respectively (Fig. 1).

134   **T**o investigate **the functionality of the** p.Gly176Trp and **the** p.Arg196del mutations **in**
135 Bos1, we used a negative selection assay as described previously (Corbett et al., 2011).
136 Since the *bos1Δ* strain of *Saccharomyces cerevisiae* is not viable, a BY4742 wild type strain
137 was transformed with pRS316-*BOS1* followed by *BOS1* deletion to generate the endogenous
138 *bos1Δ* knockout. Transformation with pRS315 plasmids encoding for Bos1 wild type or Bos1
139 mutants followed by plating on media containing 5-FOA allows for selection against pRS316
140 (Fig. 2A). Expression of the Bos1 p.Gly176Trp mutant completely perturbed growth after 48 h
141 and conferred only a little growth after 72 h when compared to wild type Bos1 indicating a
142 very severe, but not complete loss of function as was reported previously (Corbett et al.,
143 2011). Next, we substituted the glycine residue at position 176 for a hydrophilic aspartate to
144 test the importance of the presence of a hydrophobic amino acid in the -3 layer. Yeasts
145 expressing the p.Gly176Asp mutation also displayed complete perturbation of growth,
146 suggesting that either a bulky hydrophobic as well as a hydrophilic amino acid at this position
147 severely affect Bos1 function (Fig. 2A). By contrast, examination of the deletion of arginine

4

148   196 revealed only a slight growth perturbation after 48 and 72 h indicating a less severe loss
149   of function for this mutation.

150   To analyze the severity of these mutations on yeast growth more precisely and to avoid
151   toxic side effects of 5-FOA, we transformed a temperature sensitive yeast strain with the
152   different Bos1 variants (Andag et al., 2001). At 24°C the negative control showed reduced
153   growth due to temperature sensitivity, whereas expression of wild type Bos1 **was** able to
154   rescue growth (Fig. 2B). Examination of yeasts expressing the p.Gly176Trp or the
155   p.Gly176Asp mutation revealed significantly less growth than the strain carrying wild type
156   Bos1. The p.Arg196 deletion conferred comparable growth to the yeast strain transformed
157   with wild type Bos1 at 24°C. Increasing the temperature to 30°C resulted in an almost
158   complete defect in growth of yeasts expressing the -3 layer mutations p.Gly176Trp or
159   p.Gly176Asp while only a slight decrease of growth for yeast carrying the p.Arg196 deletion
160   was detected relative to wild type (Fig. 2B). Further**more**, at 37°C yeasts expressing the
161   p.Arg196del mutation displayed defective growth while yeasts transformed with wild type
162   Bos1 were still able to thrive. Next, we aimed to analyze whether p.Lys164 compared to
163   p.Arg196, in GOSR2 and Bos1 respectively, behaved similarly. Additionally, we wanted to
164   examine whether an amino acid with a smaller side chain p.Gly176Ala (rather than a large
165   Trp or Asp) in the -3 layer can be tolerated. Therefore, we expressed Bos1 p.Arg196Lys and
166   p.Gly176Ala variants in the temperature-sensitive Bos1 strain **and detected** similar growth
167   for both variants and wild type Bos1 (Fig. S1), **strongly suggesting** that these amino acid
168   substitutions are functionally redundant at these positions.

169

170 **Altered assemblies of SNARE complexes containing the Bos1 p.Gly176Trp or**
171 **p.Arg196del mutations**

172   The reduced, but not complete loss of function of the mutant Bos1 p.Gly176Trp and
173   p.Arg196del in yeast growth experiments suggests that SNARE complex function is impaired
174   but likely not completely abolished. Since SNARE complex assembly is a prerequisite for
175   SNARE-mediated fusion of membranes, we analyzed the assembly properties of the ER-to-
176   Golgi SNARE complex formed by Bos1, Bet1, Sed5 and Sec22 **using** fluorescence
177   anisotropy measurements and size exclusion chromatography (SEC). We then compared the
178   assembly behavior of the complex carrying wild type Bos1 to complexes containing the Bos1
179   p.Gly176Trp and p.Arg196del mutations. SEC experiments revealed that both the wild type
180   Bos1 or the Bos1 SNARE domains carrying the two PME associated mutations p.Gly176Trp
181   and p.Arg196del or the designed p.Gly176Asp mutation, were able to assemble into
182   complexes (Fig. S2). To examine the kinetics of Bos1 p.Gly176Trp and p.Arg196del
183   assembling with Sec22, Sed5, and Bet1, we used fluorescence anisotropy measurements.
184   This analysis allows the examination of SNARE complex formation *in vitro* using the isolated

185 SNARE domains only, as described previously (Demircioglu et al., 2014). As expected, an
186 increase of anisotropy of the labeled SNARE domain of Sec22 upon mixing with the SNARE
187 domains of the respective complex partners (Bet1, Sed5 and Bos1) was detected,
188 demonstrating the kinetics of SNARE complex assembly (Fig. 3A). Examination of the
189 kinetics of complex formation for the p.Arg196del mutant revealed a slower rate of assembly.
190 Interestingly, the p.Gly176Trp mutation induced a strongly augmented rate of assembly
191 compared to wild type Bos1. **Taken t**ogether these data indicate that both mutants are able
192 to form SNARE complexes (Fig. 3A). To further dissect the faster SNARE complex formation
193 kinetics of Bos1 carrying the p.Gly176Trp mutation, we also analyzed the p.Gly176Asp
194 mutation, since this substitution resulted in a similar attenuation of growth in yeast. In
195 contrast to the p.Gly176Trp variant, complex formation of the Bos1 p.Gly176Asp variant was
196 severely reduced when measured by the fluorescence anisotropy assay (Fig. 3A). These
197 data suggest that the introduction of a hydrophilic amino acid at the p.Gly176 position has a
198 profound effect on the speed of SNARE complex assembly.

199   Next, we wanted to understand the faster kinetics of SNARE complex assembly for the
200 Bos1 p.Gly176Trp **mutant**. Therefore, we analyzed the effects of Bos1 mutations on homo-
201 oligomer assembly using size exclusion chromatography of the purified SNARE domains.
202 Analysis of the p.Gly176Asp and p.Arg196del mutations revealed a significant propensity to
203 form oligomers which was similar to wild type Bos1. In contrast the retention volume of Bos1
204 p.Gly176Trp was largely increased (Fig. 3B), strongly suggesting that the oligomerization
205 capacity of the p.Gly176Trp was significantly reduced. These data suggest that the increased
206 rate of SNARE complex formation may be a result of the reduced propensity of the
207 p.Gly176Trp mutation to form homo-oligomers, thereby increasing the number of monomeric
208 Bos1 available for assembly.

209

210 **In silico simulation of PME mutations in GOSR2/Bos1 reveal disturbances in the**
211 **SNARE complex.**
212   Our results indicate that Bos1 p.Gly176Trp and p.Arg196del are able to assemble into
213 SNARE complexes with Sed5, Sec22 and Bet1, whereas the p.Gly176Asp mutation
214 displayed severely attenuated complex formation. As there is no crystal structure available
215 for this particular SNARE complex, we modelled the quaternary yeast and human ER-to-
216 Golgi SNARE complex using available SNARE complex structures as template. These
217 homology models were then explored by molecular dynamics (MD) simulations (Fig. 4). Our
218 results reveal that the wild type model of the assembled quaternary complexes remained
219 stable within a 10^2 ns timescale, as shown by root mean square deviation (RMSD) profiles
220 (Fig. S3A). Comparable results were obtained when we used existing X-ray structures of
221 SNARE complexes (data not shown), corroborating the robustness of our SNARE complex

222   models. We next simulated with MD complexes carrying the Bos1 p.Gly176Trp or
223   p.Arg196del mutations and the human orthologues which previous results have shown to be
224   capable of complex formation (Fig. S2). Both PME mutations behaved similar to the wild type
225   protein as both showed similarly stable RMSD values, suggesting that the mutated SNARE
226   complex**es are** stable in the explored timescale (Fig. S3A). Next, we analyzed secondary
227   structure alterations during simulations. As depicted in Fig. S3B, the SNARE complex
228   bearing the Bos1 p.Gly176Trp mutation and the human orthologue showed no strong
229   alterations in secondary structure. However, we observed small changes in the N-terminal
230   region, bearing the GOSR2 p.Gly144Trp mutation. In contrast, the complexes carrying the
231   Bos1 p.Arg196del or GOSR2 p.Lys164del mutation exhibited a local loss of helical structure,
232   likely due to the lack of helical periodicity (Fig. S3B).

233   Although complexes containing mutated Bos1 or GOSR2 remained stable during
234   prolonged MD simulations the structures appeared to exhibit local structural disturbances.
235   We investigated the regions immediately surrounding the mutations in more detail. We noted
236   that the -3 layer containing the p.Gly176Trp exchange is highly asymmetric. In addition to the
237   glycine from Bos1, the -3 layer is composed of a methionine from Sec22, a phenylalanine
238   from Sed5, and a serine from Bet1. As expected, the substitution of the small and highly
239   conserved glycine to a bulky tryptophan makes it difficult to pack all four side chains of this
240   layer into the core of the complex. Our MD simulations reveal that adjacent residues
241   opposing Trp176 in the hydrophobic layer avoided steric clashes and repeatedly evaded the
242   hydrophobic core of -3 layer, getting more solvent-accessible (Fig. 4A). Similar results were
243   obtained for the mutation of the -3 layer of the orthologous human complex, which has the
244   same amino acid composition (Fig. 4A). This observation is consistent with our yeast growth
245   experiments where the substitution of glycine for another small residue, an alanine, did not
246   lead to growth impairment (Fig. S1), whereas substitution to a large tryptophan led to a clear
247   growth defect (Fig. 2).

248   The deletion of the arginine residue at position 196 of Bos1 or the lysine residue at
249   position 164 of GOSR2 had a different effect on the assembled SNARE complex. Our MD
250   simulations showed that the deletion was surprisingly well tolerated in the assembled four-
251   helix bundle structure, although it produces a significant discontinuity of the coiled-coil
252   heptad repeat and tighter local winding (Fig. 4B). In contrast to the Gly176Trp mutation, we
253   did not observe a significant change in the solvent accessible surface area (SASA) of the
254   adjacent residues contributing to the hydrophobic core during simulations (Fig. S3C). It is
255   possible that the p.Arg196del does not affect the hydrophobic core of the complex, but
256   changes the arrangement of residues that shield the interior of the bundle and alters
257   hydrogen bonding. In the wild type complex, the deleted arginine residue at position 196 is
258   involved in stable hydrogen bond formation with an aspartate residue at position 299 in Sed5

259   (Fig. 4B). Comparison of the distribution of hydrogen bonds between Bos1 and Sed5 showed

260   that the hydrogen bond network was affected by the deletion of the p.Arg196 residue, likely

261   as a result of reduced numbers of contacts between the two neighboring SNARE helices

262   (Fig. 4B).

263   In summary, we have shown by using the orthologous yeast ER-to-Golgi SNARE

264   complex that the pathogenic mutations p.Gly144Trp and p.Lys164del in the Q_b SNARE

265   GOSR2 do not interfere with general SNARE complex stability. However, the p.Gly144Trp

266   mutation in the -3 layer appears to disturb the stability and solvent accessibility of the

267   hydrophobic core of the SNARE complex, while the p.Lys164del mutation perturbs hydrogen

268   bonding between GOSR2 and Syntaxin 5. Finally, yeast growth experiments demonstrate

269   that the p.Gly144Trp mutation causes a more severe phenotype than the p.Lys164del

270   mutation, which corresponds well with the progression of the disease in PME patients. Thus,

271   our data suggest that a combination of *in silico* and yeast experiments can describe at a

272   molecular level the assembly and stability of variant SNARE complexes.

273

Discussion

275   GOSR2 is a Q_b-SNARE protein involved in ER-to-Golgi trafficking, which is associated with

276   PME. In the present study, we investigated the functionality of the PME associated GOSR2

277   mutations p.Gly144Trp and p.Lys164del using yeast orthologues.

278   Yeasts carrying the orthologous p.Arg196del mutation of Bos1 showed growth defects at

279   elevated temperatures typical for a temperature sensitive strain. This finding suggests that

280   the function of mutated Bos1 and the orthologous mutation in GOSR2 p.Lys164del is

281   impaired but not lost. In contrast, the Bos1 p.Gly176Trp (GOSR2 p.Gly144Trp) mutation led

282   to a more significant impairment of function in yeast as indicated by severely impaired growth

283   even at lower temperatures. These results are consistent with the milder disease phenotype

284   observed in the patient carrying the compound heterozygous p.Lys164del and p.Gly144Trp

285   mutations, compared to patients homozygous for the p.Gly144Trp mutation (Boisse Lomax et

286   al., 2013, Praschberger et al., 2015).

287   Physical simulations of protein complexes indicate that the p.Gly144Trp mutation affects

288   the stability of the hydrophobic core, which provides the driving force for SNARE complex

289   formation. The substitution of the small glycine to a large tryptophan causes steric clashes

290   that might interfere with assembly of the four-helix bundle, but might also destabilize the

291   entire complex, thereby reducing its vesicle fusion activity. Notable, the p.Gly144Trp

292   mutation is in close proximity to a site important for v-SNARE binding (Pobbati et al., 2006,

293   Wiederhold and Fasshauer, 2009). Highly decelerated complex formation of p.Gly176Asp but

294   acceleration of the p.Gly176Trp variant is contrary to the expectations for impaired SNARE

295 function. However, we found that the glycine to tryptophan substitution also changed the
296 oligomeric state of Bos1 in our in vitro assembly experiments. While the isolated SNARE
297 domain of wild-type Bos1 was present as an oligomer, which needs to dissociate first for
298 SNARE complex formation, Bos1 p.Gly176Trp was already present as reactive monomer. It
299 is unlikely though that oligomerization of the SNARE domain of Bos1 plays a role during
300 SNARE complex formation in vivo.

301 According to our data, microdeletion of Lys164 did not affect the hydrophobic core, but
302 reduced the occupancy of particular hydrogen bonds between Q_a and Q_b helices. This
303 microdeletion led to a slightly destabilized alpha helix in the second half of the complex. This
304 has a less significant impact on complex assembly, as the N-terminal part contributes more
305 to complex assembly (Pobbati et al., 2006). This is supported by fluorescence anisotropy
306 measurements which displayed only slightly slowed complex assembly of Bos1 p.Arg196del
307 with its SNARE partners Sed5, Bet1 and Sec22, compared to wild type Bos1. The effect of
308 the deletion was far less severe than observed for the p.Gly176Asp variant. Although the
309 deletion does not impinge on the stability of the hydrophobic core, it might still affect the
310 membrane fusion activity of the assembled complex, because of the tighter local winding of
311 the Q_b-helix close to the transmembrane region.

312 In summary, our study provides an analysis of PME associated GOSR2 mutations *in*
313 *silico* and *in vitro*. We show that the mild**er** course of disease in a compound heterozygous
314 **PME patient** for GOSR2 p.Gly144Trp and p.Lys164del, when compared to patients
315 homozygous for GOSR2 p.Gly144Trp, is due to less severe impairment of SNARE function
316 by the p.Lys164del mutations. We also investigated SNARE function on the molecular level
317 and show**ed** that p.Gly144Trp interfere**d** with the SNARE hydrophobic core**, whereas the**
318 **p.Lys164del mutation perturbed hydrogen bond formation between GOSR2 and**
319 **Syntaxin 5.** We propose that the observed SNARE complex malfunction due to both
320 mutations could result in impaired fusion of ER- and ERGIC-derived vesicles with the cis-
321 Golgi target membrane leading to a perturbation of ER-to-Golgi trafficking. In neurons, the
322 impairment of the early anterograde transport might lead to disorders like epilepsy due to
323 alterations in the regulated release of neurotransmitters, as well as the proper sorting of
324 neurotransmitter receptors at chemical synapses, providing a possible link between
325 mutations in GOSR2 and epilepsy (Giannandrea et al., 2010, Multani et al., 1994).
326
327

328   **Material and Methods**

329   *Material*

330   If not stated otherwise, chemicals were obtained from Merck (Darmstadt, Germany), Roth

331   (Karlsruhe, Germany), Thermo Fisher Scientific (Bremen, Germany) or Sigma-Aldrich

332   (Steinheim, Germany).

333

334   *Yeast strains and negative selection with 5-FOA*

335   Yeast strains and plasmids used in this study are described in Table S1. The BY4742 *bos1Δ*

336   strain was generated by transformation of BY4742 with pRS316-*BOS1*. The resulting strain

337   was transformed with *bos1* deletion cassettes produced by PCR to achieve the endogenous

338   *bos1* deletion as previously described (Corbett et al., 2011). BY4742 *bos1Δ* strains

339   containing pRS316-*BOS1* and pRS315-plasmids expressing Bos1, Bos1 p.Gly176Trp, Bos1

340   p.Gly176Asp or Bos1 p.Arg196del were grown for 12 hours in standard minimal medium with

341   appropriate supplements (SD-Leu/Ura). Equal ODs with serial dilutions (1:10) were plated on

342   SD-Leu/Ura or SD-Leu containing 5-fluoroorotic acid (5-FOA) and incubated at 30°C for 48

343   hours. Plating of the indicated yeast strains on media containing 5-FOA allowed for negative

344   selection regarding pRS316.

345

346   *Yeast strains and survival assay of temperature-sensitive yeast strain*

347   Yeast strains and plasmids used in this study are described in Table S1. The temperature

348   sensitive (ts) yeast strain *bos1 ts* S32G-8A (Andag et al., 2001) cannot thrive at 30°C or

349   higher temperatures, unless a functional copy of Bos1 is transformed and expressed. The

350   *bos1 ts* strains containing pRS315-plasmids expressing Bos1, Bos1 p.Gly176Trp, Bos1

351   p.Gly176Asp or Bos1 p.Arg196del was grown for 12 hours in standard minimal medium with

352   appropriate supplements (SD-Leu). Equal ODs with serial dilutions (1:10) were plated on SD-

353   Leu and incubated at 24°C, 30°C, 37°C for 48 hours or room temperature for 72 hours. Only

354   yeast strains which express a functional copy of Bos1 can rescue the temperature sensitive

355   phenotype of the *bos1 ts* strain at 30°C and 37°C.

356

357   *Protein Constructs and Purification*

358   Plasmids used in this study are listed in Table S2. Unlike Bet1, only the SNARE domains of

359   Sed5, Sec22 and Bos1 were expressed. Single-cysteine variants used in this study were

360   designed as previously described (Demircioglu et al., 2014). Recombinant proteins were

361   expressed in *Escherichia coli* strain BL21 (DE3) and purified by Ni^{2+}-NTA chromatography

362   followed by ion exchange chromatography on an Äkta system (GE Healthcare, Solingen,

363   Germany). Depending on the pI of each protein, MonoQ or MonoS was used as ion

364   exchanger. Protein elution was performed by using a linear gradient of NaCl in 20 mM Tris,

365 pH 7.4 buffer containing 1 mM EDTA and additionally 1 mM DTT for proteins carrying
366 cysteine residues. Hexa-His tags were removed before ion exchange chromatography via
367 thrombin cleavage. Protein concentrations were determined by absorption at 280 nm or
368 using Bradford Assay.
369

370 *Fluorescence anisotropy*
371 Fluorescence measurements were performed in a spectrofluorometer equipped with a
372 second emission channel in T-configuration (QuantaMaster 40, PTI, Birmingham, NJ 08011).
373 Sec22 126-186^{D131C} was labeled with Oregon Green (OG) 488 iodoacetamide according to
374 manufacturer´s protocol and protein concentration determined via Bradford assay.
375 Experiments were carried out in 1 cm quartz cuvettes (Hellma, Müllheim, Germany) in PBS
376 buffer at 25°C. Measurement of fluorescence anisotropy, which increases upon complex
377 formation due to local flexibility of the labeled residue, was carried out as previously
378 described (Burkhardt et al., 2008).
379

380 *Size exclusion chromatography*
381 The oligomeric state of single proteins and quaternary SNARE complexes was analyzed by
382 size exclusion chromatography on a Superdex 75 column in PBS buffer containing 200 mM
383 NaCl. Quaternary SNARE complexes consisting of Sed5 (211-320), Bet1 (1-118), Sec22
384 (126-186) and one of the Bos1 (151-221) variants were assembled with equal amounts of
385 purified components and incubated overnight in PBS buffer containing 200 mM NaCl. The
386 molecular weight was calculated with a standard containing Dextran blue, BSA, ovalbumine,
387 cytochrome c and aprotinin.
388
389 *Modeling and molecular dynamics simulations of the SNARE complexes*
390 A set of crystal structures of different SNARE complexes (PDB ID codes 2NPS, 2GL2, 1SFC,
391 3B5N, 4WY4) was used as templates for modeling (Welch et al., 2012). Models of human
392 and yeast complexes were generated with Modeller v.9 (Sali and Blundell, 1993). Each
393 complex was prepared for simulations using the Leap module of AmberTools (Schafmeister
394 et al., 1995). Simulations were run with the NAMD engine (Phillips et al., 2005) using the
395 AMBER99SBildn force field (Hornak et al., 2006) and TIP3P parameters for water
396 (Jorgensen et al., 1983). Standard sodium and chloride parameters from the AMBER force
397 field were used. A conservative cutoff of 12 Å (Piana et al., 2012) was set for nonbonded
398 interactions with a switching function active between 10 Å and 12 Å. Electrostatics were
399 treated through particle-mesh Ewald summations with a grid spacing of 1 Å. Each simulation
400 box was minimized, equilibrated by Cα-restrained heating in 10 steps of 30 K up to 300 K for
401 a total of 1 ns, and further equilibrated by unrestrained heating. Subsequently, the production

402 simulations were carried out at 300 K and 1 atm, controlled with a Nosé–Hoover Langevin
403 piston.
404 Models of human and yeast complexes after unrestrained equilibration were used as
405 templates to generate corresponding mutant complexes. After equilibration, all models were
406 simulated for 90 ns. As no significant RMSD changes were observed after the first 50 ns,
407 additional replicas were only run for 60 ns. Each system was simulated in three replicas.
408 Trajectories were analyzed with VMD software modules and Tcl scripts. For hydrogen bond
409 contact measurements a cutoff distance of 3.6 Å between heavy atoms and an angle cutoff
410 of 30° were used.
411

Acknowledgements

416

Conflict of interest

418 The authors declare no conflicts of interests.

419

Funding

424 **References**

425 Andag, U., Neumann, T. and Schmitt, H. D. (2001). The coatomer-interacting protein Dsl1p is required for
426 Golgi-to-endoplasmic reticulum retrieval in yeast. *J. Biol. Chem.,* 276, 39150-60.

427 Berkovic, S. F., Andermann, F., Carpenter, S. and Wolfe, L. S. (1986). Progressive myoclonus epilepsies:
428 specific causes and diagnosis. *The New England journal of medicine,* 315, 296-305.

429 Boisse Lomax, L., Bayly, M. A., Hjalgrim, H., Moller, R. S., Vlaar, A. M., Aaberg, K. M., Marquardt, I., Gandolfo, L.
430 C., Willemsen, M., Kamsteeg, E. J., et al. (2013). 'North Sea' progressive myoclonus epilepsy: phenotype of
431 subjects with GOSR2 mutation. *Brain : a journal of neurology,* 136, 1146-54.

432 Burkhardt, P., Hattendorf, D. A., Weis, W. I. and Fasshauer, D. (2008). Munc18a controls SNARE assembly
433 through its interaction with the syntaxin N-peptide. *The EMBO journal,* 27, 923-33.

434 Corbett, M. A., Schwake, M., Bahlo, M., Dibbens, L. M., Lin, M., Gandolfo, L. C., Vears, D. F., O'sullivan, J. D.,
435 Robertson, T., Bayly, M. A., et al. (2011). A mutation in the Golgi Qb-SNARE gene GOSR2 causes progressive
436 myoclonus epilepsy with early ataxia. *Am J Hum Genet,* 88, 657-63.

437 Crooks, G. E., Hon, G., Chandonia, J. M. and Brenner, S. E. (2004). WebLogo: a sequence logo generator.
438 *Genome Res.,* 14, 1188-90.

439 Demircioglu, F. E., Burkhardt, P. and Fasshauer, D. (2014). The SM protein Sly1 accelerates assembly of the
440 ER-Golgi SNARE complex. *Proceedings of the National Academy of Sciences of the United States of America,*
441 111, 13828-33.

442 Fasshauer, D., Sutton, R. B., Brunger, A. T. and Jahn, R. (1998a). Conserved structural features of the
443 synaptic fusion complex: SNARE proteins reclassified as Q- and R-SNAREs. *Proc. Natl. Acad. Sci. U. S. A.,* 95,
444 15781-6.

445 Fasshauer, D., Sutton, R. B., Brunger, A. T. and Jahn, R. (1998b). Conserved structural features of the
446 synaptic fusion complex: SNARE proteins reclassified as Q- and R-SNAREs. *Proceedings of the National*
447 *Academy of Sciences of the United States of America,* 95, 15781-6.

448 Giannandrea, M., Bianchi, V., Mignogna, M. L., Sirri, A., Carrabino, S., D'elia, E., Vecellio, M., Russo, S., Cogliati,
449 F., Larizza, L., et al. (2010). Mutations in the small GTPase gene RAB39B are responsible for X-linked mental
450 retardation associated with autism, epilepsy, and macrocephaly. *American journal of human genetics,* 86, 185-95.

451 Gordon, D. E., Bond, L. M., Sahlender, D. A. and Peden, A. A. (2010). A targeted siRNA screen to identify
452 SNAREs required for constitutive secretion in mammalian cells. *Traffic (Copenhagen, Denmark),* 11, 1191-204.

453 Hay, J. C., Chao, D. S., Kuo, C. S. and Scheller, R. H. (1997). Protein interactions regulating vesicle transport
454 between the endoplasmic reticulum and Golgi apparatus in mammalian cells. *Cell,* 89, 149-58.

455 Hay, J. C., Klumperman, J., Oorschot, V., Steegmaier, M., Kuo, C. S. and Scheller, R. H. (1998). Localization,
456 dynamics, and protein interactions reveal distinct roles for ER and Golgi SNAREs. *The Journal of cell biology,*
457 141, 1489-502.

458 Hornak, V., Abel, R., Okur, A., Strockbine, B., Roitberg, A. and Simmerling, C. (2006). Comparison of multiple
459 Amber force fields and development of improved protein backbone parameters. *Proteins,* 65, 712-25.

460 Jahn, R. and Scheller, R. H. (2006). SNAREs--engines for membrane fusion. *Nature reviews. Molecular cell*
461 *biology,* 7, 631-43.

462 Jorgensen, J. L., Chandrasekhar, J., Madura, J. D., Impey, R. W. and Klein, M. L. (1983). Comparison of
463 simple potential functions for simultating liquid water. *J. Chem. Phys.,* 79, 926-935.

464 Kloepper, T. H., Kienle, C. N. and Fasshauer, D. (2007). An elaborate classification of SNARE proteins sheds
465 light on the conservation of the eukaryotic endomembrane system. *Mol. Biol. Cell,* 18, 3463-71.

466 Lowe, S. L., Peter, F., Subramaniam, V. N., Wong, S. H. and Hong, W. (1997). A SNARE involved in protein
467 transport through the Golgi apparatus. *Nature,* 389, 881-4.

468 Multani, P., Myers, R. H., Blume, H. W., Schomer, D. L. and Sotrel, A. (1994). Neocortical dendritic pathology
469 in human partial epilepsy: a quantitative Golgi study. *Epilepsia,* 35, 728-36.

470 Parlati, F., Mcnew, J. A., Fukuda, R., Miller, R., Sollner, T. H. and Rothman, J. E. (2000). Topological
471 restriction of SNARE-dependent membrane fusion. *Nature,* 407, 194-8.

472 Phillips, J. C., Braun, R., Wang, W., Gumbart, J., Tajkhorshid, E., Villa, E., Chipot, C., Skeel, R. D., Kale, L. and
473 Schulten, K. (2005). Scalable molecular dynamics with NAMD. *J. Comput. Chem.,* 26, 1781-802.

474 Piana, S., Lindorff-Larsen, K., Dirks, R. M., Salmon, J. K., Dror, R. O. and Shaw, D. E. (2012). Evaluating the
475 effects of cutoffs and treatment of long-range electrostatics in protein folding simulations. *PLoS One,* 7, e39918.

476 Pobbati, A. V., Stein, A. and Fasshauer, D. (2006). N- to C-terminal SNARE complex assembly promotes rapid
477 membrane fusion. *Science,* 313, 673-6.

478 Praschberger, R., Balint, B., Mencacci, N. E., Hersheson, J., Rubio-Agusti, I., Kullmann, D. M., Bettencourt, C.,
479 Bhatia, K. and Houlden, H. (2015). Expanding the Phenotype and Genetic Defects Associated with the GOSR2
480 Gene. *Movement Disorders Clinical Practice,* 2, 271-273.

481 Sali, A. and Blundell, T. L. (1993). Comparative protein modelling by satisfaction of spatial restraints. *J. Mol. Biol.,*
482 234, 779-815.

483 Schafmeister, C. E. a. F., Ross, W. S. and Romanovski, V. (1995). *LeaP.*, University of California, San Francisco.

484 Sprecher, E., Ishida-Yamamoto, A., Mizrahi-Koren, M., Rapaport, D., Goldsher, D., Indelman, M., Topaz, O.,
485 Chefetz, I., Keren, H., O'brien T, J., et al. (2005). A mutation in SNAP29, coding for a SNARE protein involved
486 in intracellular trafficking, causes a novel neurocutaneous syndrome characterized by cerebral dysgenesis,
487 neuropathy, ichthyosis, and palmoplantar keratoderma. *American journal of human genetics,* 77, 242-51.

488 Sutton, R. B., Fasshauer, D., Jahn, R. and Brunger, A. T. (1998). Crystal structure of a SNARE complex
489 involved in synaptic exocytosis at 2.4 A resolution. *Nature,* 395, 347-53.

14

490   Welch, B. D., Liu, Y., Kors, C. A., Leser, G. P., Jardetzky, T. S. and Lamb, R. A. (2012). Structure of the
491   cleavage-activated prefusion form of the parainfluenza virus 5 fusion protein. *Proc. Natl. Acad. Sci. U. S. A.,* 109,
492   16672-7.

493   Wiederhold, K. and Fasshauer, D. (2009). Is assembly of the SNARE complex enough to fuel membrane
494   fusion? *J. Biol. Chem.,* 284, 13143-52.

495   Xu, D., Joglekar, A. P., Williams, A. L. and Hay, J. C. (2000). Subunit structure of a mammalian ER/Golgi
496   SNARE complex. *The Journal of biological chemistry,* 275, 39631-9.

497   Zur Stadt, U., Schmidt, S., Kasper, B., Beutel, K., Diler, A. S., Henter, J. I., Kabisch, H., Schneppenheim, R.,
498   Nurnberg, P., Janka, G., et al. (2005). Linkage of familial hemophagocytic lymphohistiocytosis (FHL) type-4
499   to chromosome 6q24 and identification of mutations in syntaxin 11. *Human molecular genetics,* 14, 827-34.

Figures

501 **Figure 1: SNARE motif sequence alignment of GOSR2 and its yeast orthologue Bos1.**

502 The PME associated mutations of GOSR2, p.Gly144 and p.Lys164, as well as the yeast
503 orthologue Bos1 p.Gly176 and p.Arg196 are located at highly conserved positions within the
504 SNARE motif. GOSR2 and Bos1 contain an N-terminal Habc domain, a SNARE motif and a
505 transmembrane domain at the C-terminus. Sequence alignments of SNARE proteins of over
506 200 animals or fungi are presented as weblogo show the high sequence conservation of the
507 SNARE domain (Crooks et al., 2004). GOSR2 and Bos1 share high sequence similarity. The
508 SNARE motif consists of 16 hydrophobic layers as indicated. The p.Gly144 and p.Gly176 are
509 located at the -3 layer, whereas p.Lys164 and p.Arg196 are located between layers +2 and
510 +3 (Kloepper et al., 2007).

511

512 **Figure 2: The effect of Bos1 mutations on yeast growth.**

513 (A) Bos1 p.Gly176Trp, p.Gly176Asp and p.Arg196del show growth impairment compared to
514 Bos1 wild type. The yeast strain BY4742 *bos1Δ* containing pRS316-*BOS1* was generated as
515 previously described (Corbett et al., 2011) and transformed with pRS315-plasmids
516 expressing Bos1 wild type or Bos1 mutants. URA3, which is only present on the pRS316
517 plasmid, converts 5 fluoroorotic acid (5-FOA) to cytotoxic 5-fluorouracil. Plating yeast cells on
518 media containing 5-FOA allows for negative selection regarding RS316. Only cells that
519 express a functional Bos1 protein and lack pRS316 can thrive on 5-FOA containing media.
520 Indicated strains were spotted on SD-Leu/Ura and 5-FOA plates with serial dilutions (1:10)
521 and incubated at 30°C for 48 hours. Cells transfected with pRS315-*bos1*-p.Arg196del
522 showed impaired growth compared to pRS315-*BOS1* wild type strains, however pRS315-
523 *bos1*-p.Gly176Trp and –p.Gly176Asp led to severe impairment indicating a functional
524 impairment of the Bos1 p.Arg196del mutant and even stronger of the Bos1 p.Gly176Trp and
525 p.Gly176Asp variants. (B) Temperature sensitive strain of *Saccharomyces cerevisiae* was
526 transformed with different variants of Bos1. At room temperature, growth was detected for all
527 variants including the negative control. At 24°C, reduced growth was detected for Bos1
528 p.Gly176Trp and p.Gly176Asp; only few remaining colonies were detected for the negative
529 control. At 30°C, only the wild type and the p.Arg196del enabled the yeast to grow. Finally, at
530 37°C, also yeasts transformed with the p.Arg196del variant lacked the ability to grow
531 completely.

532 **Figure 3: ER-Golgi SNARE complex formation with Bos1 p.Arg196del.**

533 (A) SNARE complex formation was measured by the increase of fluorescence anisotropy as
534 previously described (Demircioglu et al., 2014). For assembly, 500 nM OG-labeled Sec22

535 126-186^{C131OG} were mixed with 2.7 µM Sed5 211-320, Bet1 1-118 and Bos1 151-221 or its

536 mutants. A slower increase in fluorescence anisotropy indicates a reduced capability of Bos1

537 p.Arg196del to form the ER-Golgi SNARE complex. Bos1 p.Gly176Asp shows an even

538 stronger effect. However, complex formation of Bos1 p.Gly176Trp seems to be accelerated.

539 (B) Size exclusion chromatography was performed for the individual SNARE domains of

540 Bos1 variants. The Bos1 variants wild type, p.Gly176Asp and p.Arg196del seemed to be

541 present in a higher oligomeric state than Bos1 p.Gly176Trp.

542 **Figure 4: In silico simulation of the SNARE complexes bearing the two PME mutations.**

543 Molecular dynamics (MD) simulations suggest that the impact of proteins bearing mutated

544 residues on the SNARE complex is different. (A) MD simulations of models of the quaternary

545 yeast and human ER-to-Golgi SNARE complexes revealed that the Gly144Trp mutation of

546 GOSR2 as well as the orthologues Gly176Trp mutation of Bos1 interfered with the integrity of

547 the hydrophobic core of the helix bundle in the region surrounding layer -3, visible by an

548 increase of the solvent accessible surface area (SASA). Plotted are independent MD

549 replicas. (B) The deletion of Lys164 in GOSR2 or Arg196 in Bos1 led to a slight impairment

550 of the hydrogen bond network between Qa and Qb helices. On the right, relative H-bond

551 occupancy for different H-bonds between the neighboring Q_a- and Q_b-helices is reported for

552 the different models. The different H-bonds are sorted based on their occupancy (H-bond
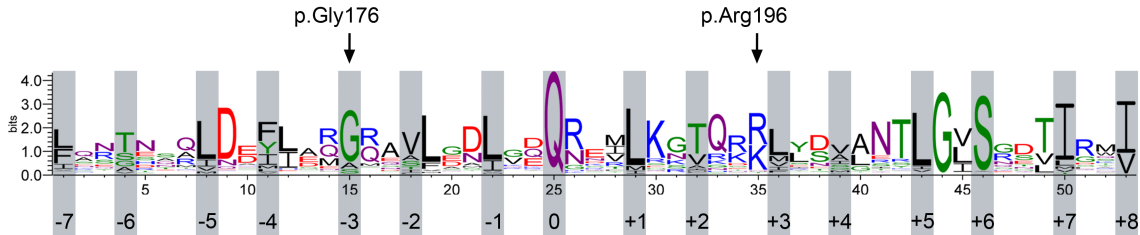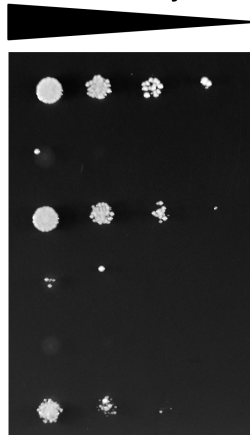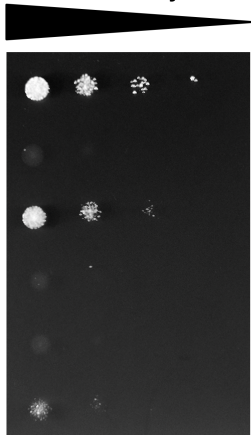
553 rank).

554

555

556
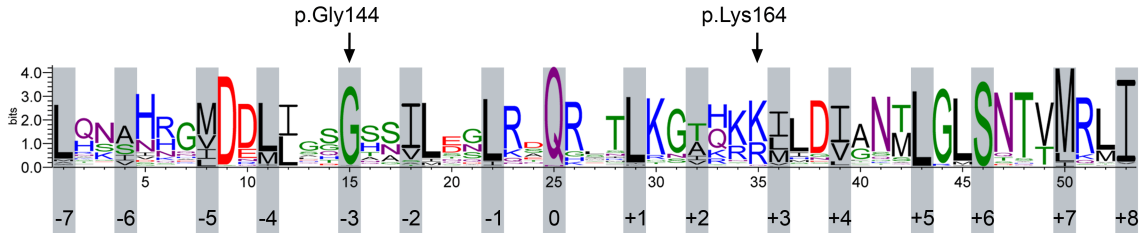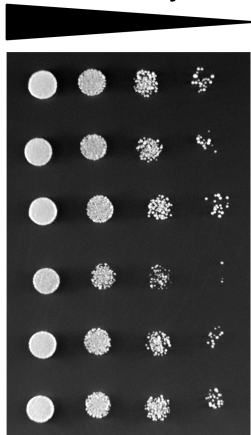
A

	SD-Leu/Ura	SD-Leu + 5-FOA	
30°C, 48 h		30°C, 48 h	30°C, 72 h

wild type + pRS315

bos1△ + pRS315

bos1△ + pRS315-*BOS1*

bos1△ + pRS315-*bos1* p.Gly176Trp

bos1△ + pRS315-*bos1* p.Gly176Asp

bos1△ + pRS315-*bos1* p.Arg196del

pRS316-*BOS1*

B
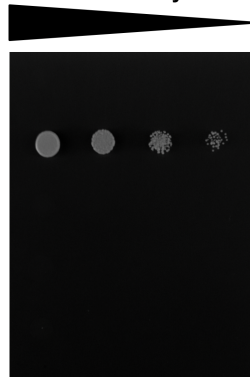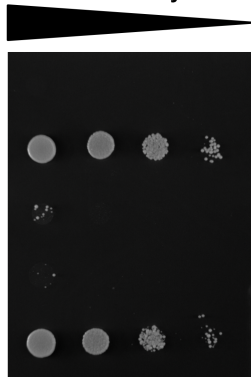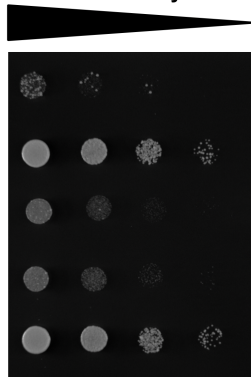
bos1 ts + pRS315

bos1 ts + pRS315-*BOS1*

bos1 ts + pRS315-*bos1* p.Gly176Trp

bos1 ts + pRS315-*bos1* p.Gly176Asp

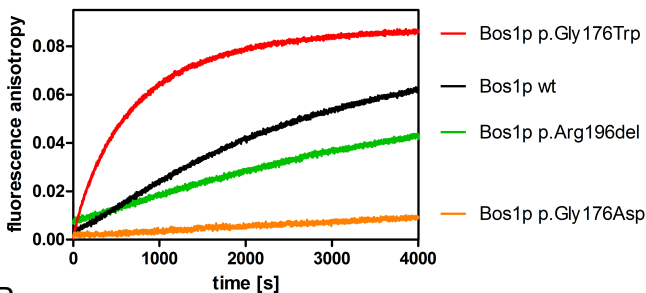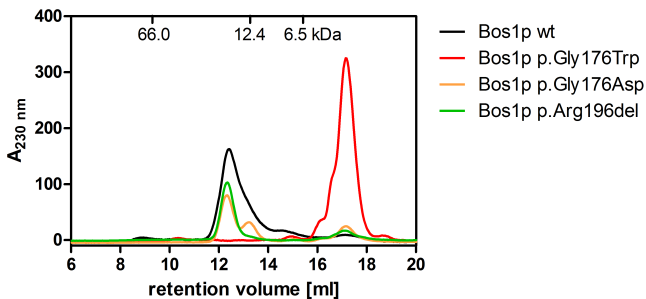bos1 ts + pRS315-*bos1* p.Arg196del

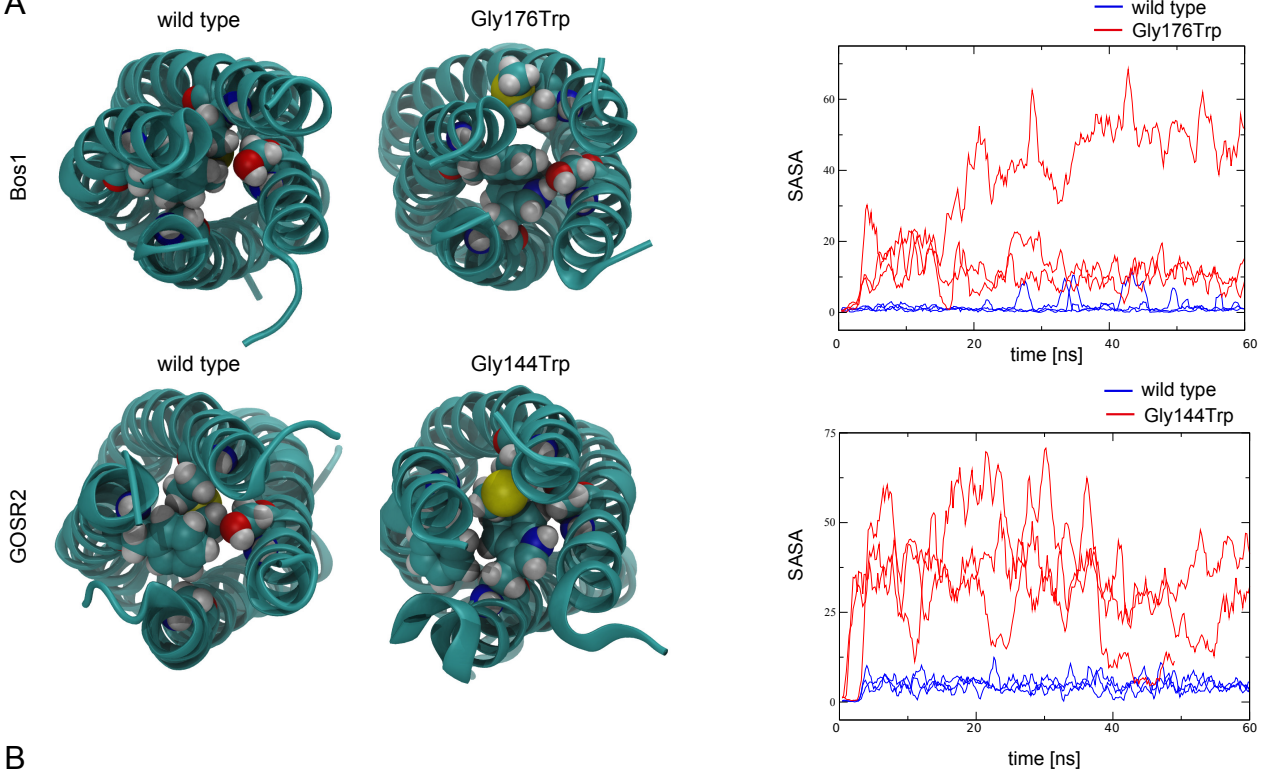24°C, 48 h   30°C, 48 h   37°C, 48 h

SD-Leu

A

fluorescence anisotropy vs time [s]

Bos1p p.Gly176Trp
Bos1p wt
Bos1p p.Arg196del
Bos1p p.Gly176Asp

B

$A_{230\ nm}$ vs retention volume [ml]

66.0   12.4   6.5 kDa

Bos1p wt
Bos1p p.Gly176Trp
Bos1p p.Gly176Asp
Bos1p p.Arg196del